RESEARCH PAPER

Design, Synthesis, Molecular Docking, and Antimicrobial Evaluation of Novel Pyrazole–Naphthalene Hybrids

Gunjan Bodwal[1], Rakesh Narang[1], Arun Kumar[1], Suman Rohilla[1*]
[1]Department of Pharmaceutical Sciences, Gurugram University, Sector 87, Pincode-122505, Gurugram, Haryana, India.
***Corresponding Author: Dr. Suman Rohilla**
Assistant Professor, Department of Pharmaceutical Sciences, Gurugram University, Gurugram, Haryana, India
Email: rh.suman@gmail.com, sumanrohilla.pharmacy@gurugramuniversity.ac.in

ABSTRACT
A new series of pyrazole–naphthalene hybrid derivatives was rationally designed, synthesized, and evaluated for their antimicrobial potential. The escalating prevalence of antimicrobial resistance and the diminishing efficacy of current therapeutics necessitate the development of new agents with improved activity profiles. Naphthalene was strategically employed as a bioisosteric substitute for the quinoline moiety of ciprofloxacin and hybridized with variously substituted pyrazole aldehydes to generate structurally diverse analogues. Target naphthalene–pyrazole derivatives (13a–g) were synthesized by condensation of pyrazole aldehydes (9a–g) with 1-naphthaleneacetic acid hydrazide (12). The synthesised compounds were screened for antibacterial and antifungal activities. Among them, compound 13d, bearing a para-chloro substituent, exhibited the most potent and broad-spectrum antibacterial activity (MIC 62.5–250 µg/mL) along with notable antifungal efficacy (MFC 250–500 µg/mL), identifying it as the most promising lead candidate. Structure–activity relationship analysis indicated that the nature and position of substituents significantly influenced antimicrobial potency. Molecular docking studies supported the biological findings, with compound 13d demonstrating the highest binding affinity (–8.6 kcal/mol) toward the target protein. Furthermore, in silico pharmacokinetic evaluation predicted favorable drug-like properties, suggesting its potential for further optimization and development as an antimicrobial agent.
Keywords: Molecular hybridization, Pyrazole–Naphthalene hybrid, Antimicrobial, Bioisosterism.
How to cite this article: Bodwal G, Narang R, Kumar A, Rohilla S. Design, Synthesis, Molecular Docking, and Antimicrobial Evaluation of Novel Pyrazole–Naphthalene Hybrids. Int J Drug Deliv Technol. 2026;16(59s): 500-506. DOI: 10.25258/ijddt.16.59s.53
Source of support: Nil
Conflict of interest: None

GRAPHICAL ABSTRACT

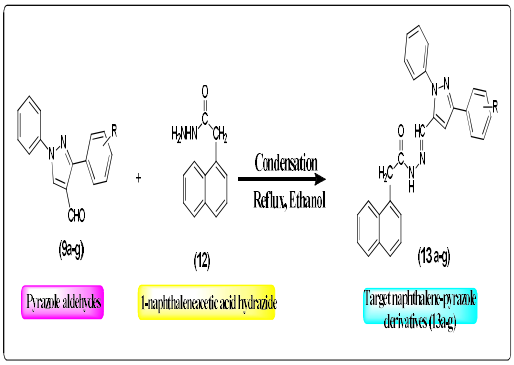

INTRODUCTION

Antimicrobial resistance (AMR) presents a serious global health threat accounting for with nearly 4.71 million mortalities in 2021, and its burden is expected to increase significantly by 2050 [1,2]. The growing prevalence of multidrug-resistant (MDR) and extensively drug-resistant (XDR) pathogens has severely limited current therapeutic options [3]. Therefore, the development of novel hybrid pharmacophores and bioisosteric modifications has become an important strategy to combat resistance. In the present work, the quinoline ring of ciprofloxacin was bioisosterically replaced with a naphthalene scaffold to retain key pharmacophoric interactions and potentially improve antibacterial activity [4]. Naphthalene, present in drugs such as nafcillin, terbinafine etc. is an important antimicrobial scaffold due to its rigid, hydrophobic, and planar structure that enhances microbial cell penetration [5]. Pyrazole, a key medicinal scaffold featured in numerous FDA-approved drugs, is also present in antibiotics such as ceftolozane and cefoselis, underscoring its clinical relevance [6-8]. By combining naphthalene with the pyrazole ring, a heterocycle with diverse biological activities including antibacterial, anti-inflammatory, and enzyme-inhibitory effects a rational naphthalene–pyrazole hybrid scaffold is designed. The designed strategy, as depicted in **Figure 1** is supported by molecular docking to predict binding interactions, *in silico* ADMET analyses to evaluate pharmacokinetics, drug-likeness, and toxicity, and *in vitro* antimicrobial assays to confirm efficacy, collectively guiding the selection of promising analogs for further development.

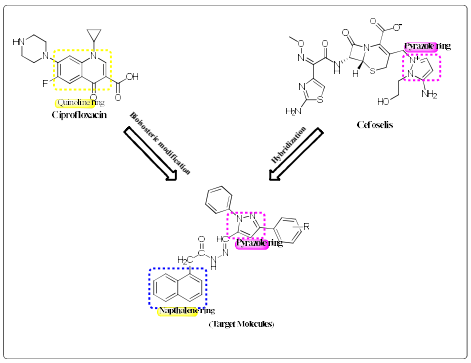

Figure 1: Molecular hybridization design strategy of naphthalene-pyrazole as new antimicrobial agents

RESULTS AND DISCUSSION

Chemistry: Hydrazone intermediates (8a–g) were synthesized from substituted acetophenones and phenylhydrazine, followed by Vilsmeier–Haack cyclization to yield pyrazole aldehydes (9a–g) as reported [9-11]. 1-Naphthaleneacetohydrazide (12) was prepared according to a reported method [12]. Finally, condensation of pyrazole aldehydes (9a–g) with hydrazide (12) afforded the target naphthalene–pyrazole hybrids (13a–g). The compound exhibits E/Z isomerism around the C=N bond, with the (E)-isomer being more stable due to reduced steric hindrance as bulky groups are on opposite sides [13].

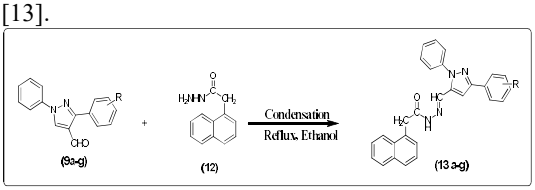

Compound	R	Compound	R
13a	H	13e	NO_2
13b	OH	13f	OCH_3
13c	Br	13g	CH_3
13d	Cl		

Scheme 1: Synthetic scheme to design naphthalene–pyrazole hybrids

Antimicrobial Activity Evaluation: Antibacterial and antifungal activities were evaluated by the microbroth dilution method to determine MIC values using standardized MTCC strains of *Escherichia coli, Pseudomonas aeruginosa, Staphylococcus aureus, Streptococcus pyogenes, Candida albicans, Aspergillus niger,* and *Aspergillus clavatus* [13]. Serial dilutions (1000–6.25 µg/mL) were prepared for screening of test compounds and IC_{50} values were noted. It was observed that all hybrids exhibited moderate to good activity, with potency varying according to substitution (**Table 1).** Compound **13d** bearing a *para*-chloro substitution showed the strongest and broad-spectrum antibacterial effect (MIC 62.5–250 µg/mL) and superior antifungal activity (MFC 250–500 µg/mL), identifying it as the most promising lead among the series. Compound **13b** and **13f** exhibited good to moderate activity, whereas compounds **13a, 13c, 13e,** and **13g** displayed comparatively weaker activity than the standards. Overall, the results indicated that the pattern of substitution significantly influenced antimicrobial efficacy, and the naphthalene–pyrazole scaffold represents a viable framework for further optimization.

Table 1: Minimum Inhibitory Concentration (MIC, µg/mL) values of the synthesized compounds **13a-g**

S No	Comp No:	Comp code	*E. coli MTCC 443*	*P. Aeruginosa MTCC 1688*	*S. aureus MTCC 96*	*S. pyogenes MTCC 442*	C. albicans MTCC 227	A. niger MTCC 282
1	13a	G1	200	250	100	62.5	1000	1000
2	13b	G2	125	100	62.5	100	500	500
3	13c	G3	100	200	125	100	1000	1000
4	13d	G4	62.5	100	200	250	250	500
5	13e	G5	200	62.5	125	200	1000	>1000
6	13f	G6	125	100	62.5	100	500	500
7	13g	G7	100	125	125	200	1000	1000
8	-	Gentamicin	0.05	1	0.25	0.5	—	—
9	-	Ampicillin	30	—	40	25	—	—
10	-	Chloramphenicol	50	50	50	50	—	—
11	-	Ciprofloxacin	25	25	50	50	—	—
12	-	Norfloxacin	10	10	10	10	—	—
13		Nystatin	—	—	—	—	100	100

14		**Griseofulvin**	—	—	—	—	500	100

***In silico* ADMET Analysis (pharmacokinetic predictions):** The pharmacokinetic properties of all the synthesized hybrids were predicted *in silico* using online freely available SwissADME tool [13]. All the structures were drawn in the ChemDraw and analysed for various key pharmacokinetic parameters including lipophilicity, solubility, GI absorption, BBB permeability, and bioavailability (**Table 2**). All hybrids (**13a-g**) showed satisfactory physicochemical properties, with molecular weights ranging 430–509 g/mol and Log P values of 3.2–4.0, indicating favorable membrane permeability. Newly synthesized hybrids exhibited number of hydrogen bond donor (HBD), hydrogen bond acceptor (HBA), rotatable bonds, and TPSA, in the permissible limits suggesting good oral absorption; only **13e** exhibited slightly higher polarity. Overall, the series demonstrated satisfactory drug-likeness and pharmacokinetic potential for further evaluation.

Table 2: *In silico* predicted pharmacokinetic properties of synthesized compounds

SNo	**Comp No**	**MW**	**Log P**	**HBD**	**HBA**	**TPSA (Å)**	**RB**
1	**13a**	430.5	3.7	1	3	59.28	7
2	**13b**	446.5	3.24	2	4	79.51	7
3	**13c**	509.4	4	1	3	59.28	7
4	**13d**	464.95	3.98	1	3	59.28	7
5	**13e**	475.5	3.31	1	5	105.1	8
6	**13f**	460.53	3.95	1	4	68.51	8
7	**13g**	444.53	3.8	1	3	59.28	7

Molecular Docking Study: Molecular docking was performed to assess the binding affinity and interaction profile of
the synthesized pyrazole–naphthalene derivatives (**13a-g**) with *E. coli* Gyrase B (PDB ID: 6F86) [21]. Docking protocol validation *via* redocking of the native ligand showed an RMSD < 2.0 Å, confirming reliability. All compounds occupied the ATP-binding pocket and formed stable interactions with key catalytic residues. Ciprofloxacin and novobiocin were used as reference drugs. The binding energies ranged from –7.3 to –8.7 kcal/mol, indicating moderate to strong affinity. Compounds **13a** (–8.7 kcal/mol) and **13d** (–8.6 kcal/mol) showed the highest affinity. Hydrogen bonding, particularly involving the pyrazole moiety and heteroatoms, was a major stabilizing factor, with residues ASN46, GLN72, THR34, THR165, and ARG190 engaged at distances of 2.9–3.2 Å. Hydrophobic and electrostatic interactions, including π–σ, π–alkyl, and π–cation contacts with residues ILE94, ASP74, LYS162, ALA147, VAL71, and ARG76, further stabilized the ligands. Compound **13a** exhibited dual H-bonds with ASN46 and multiple π–σ/π–alkyl interactions involving the pyrazole and naphthyl rings. **13b** and **13g** showed stable H-bonds with GLN72 and π–σ interactions with ASP74 and LYS162. G3 and G4 interacted mainly through the pyrazole ring with contacts at THR165 and ILE94. **13e** showed electrostatic stabilization *via* π–cation and π–alkyl interactions, while **13f** strong docking score (–8.4 kcal/mol) resulted from H-bonding through an OCH_3-substituted pyrazole and π–cation contacts with ARG76. **Figures 5-11** illustrate 2D and 3D interactions of the synthesized compounds, and Figures 12 &13 depict the standard drugs' interactions with *E. coli* Gyrase B. The docking results correlate with the observed structure–activity relationships, highlighting **13a** and **13d** as the most promising antibacterial candidates.

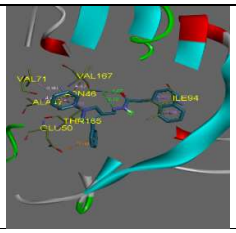

Figure 5 (a) 3D interaction diagram of compound G-1 (13a)

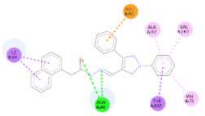

Figure 5 (b) 2D interaction diagram of compound G-1 (13a)

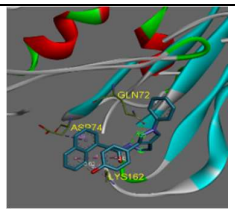

Figure 6 (a) 3D interaction diagram of compound G-2 (13b)

Figure 6 (b) 2D interaction diagram of compound G-2 (13b)

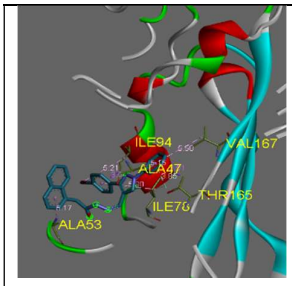

Figure 7 (a) 3D interaction diagram of compound G-3 (13c)

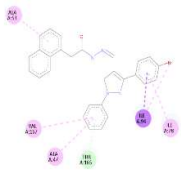

Figure 7 (b) 2D interaction diagram of compound G-3 (13c)

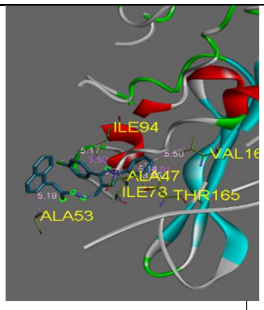

Figure 8 (a) 3D interaction diagram of compound G-4 (13d)

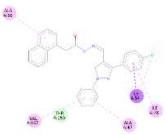

Figure 8 (b) 2D interaction diagram of compound G-4 (13d)

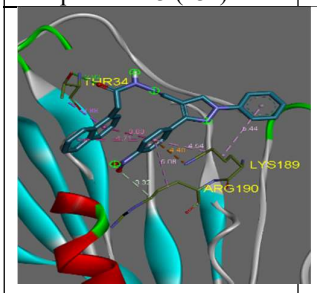

Figure 9 (a) 3D interaction diagram of compound G-5 (13e)

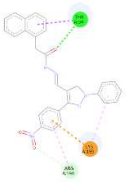

Figure 9 (b) 2D interaction diagram of compound G-5 (13e)

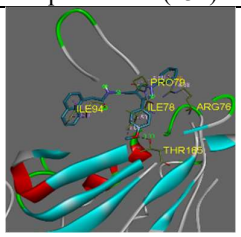

Figure 10 (a) 3D interaction diagram of compound G-6 (13f)

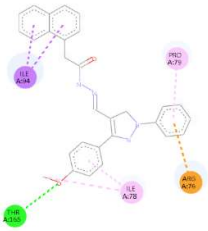

Figure 10 (b) 2D interaction diagram of compound G-7 (13f)

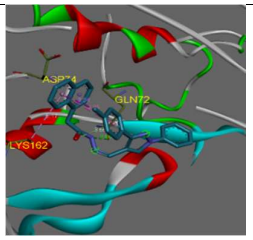

Figure 11 (a) 3D interaction diagram of compound G-7 (13g)

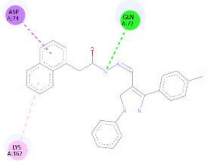

Figure 11 (b) 2D interaction diagram of compound G-7 (13g)

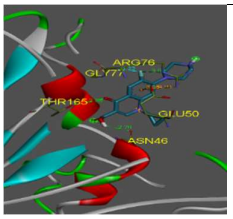

Figure 12 (a) 3D interaction diagram of Ciprofloxacin (standard)

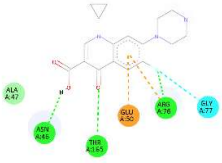

Figure 12 (b) 2D interaction diagram of Ciprofloxacin (standard)

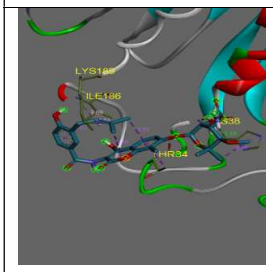

Figure 13 (a) 3D interaction diagram of Novobiocin (standard)

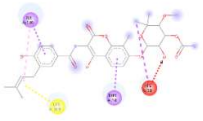

Figure 13 (b) 3D interaction diagram of Novobiocin (standard)

Figure 5(a-b)-13(a-b): 2D and 3D interaction diagram of synthesized compound (13a- 13g) and standard drugs (Ciprofloxacin & Novobiocin) with *E. coli* Gyrase B (PDB ID: 6F86)

EXPERIMENTAL

All reagents and solvents including phenylhydrazine, substituted acetophenones, phosphorus oxychloride ($POCl_3$), dimethylformamide (DMF), hydrazine hydrate, ethanol, glacial acetic acid, and sulfuric acid were of analytical grade and procured from Central Drug House, Loba Chemie, and Merck. Melting points were determined using a digital melting point apparatus. Reaction progress and purity were monitored by TLC on silica gel plates. IR spectra were recorded on an FT-IR spectrophotometer, while ^{1}H NMR spectra were obtained on a Bruker Avance III 500 MHz NMR spectrometer using TMS as internal standard. Mass spectra were recorded using ESI-MS instrumentation.

General procedure for the synthesis of hydrazone intermediates (8a–g) and pyrazole-based aldehydes (9a–g)

Hydrazone intermediates (8a–g), isolated as pale-yellow crystals, underwent cyclization/formylation with the Vilsmeier–Haack reagent to yield pyrazole-based aldehydes (9a–g) as off-white solids, which were recrystallized for purification [14].

General procedure for the synthesis of naphthalene–pyrazole derivatives (13a–g)

A mixture of the appropriate pyrazole-based aldehyde (**9a–g**) (0.01 mol) and hydrazide (**12**) (0.01 mol) in ethanol (30 ml) was refluxed for 3-4 h. After completion of the reaction, the mixture was cooled to room temperature, and the resulting solid was filtered, washed with water, and dried to afford the corresponding naphthalene–pyrazole derivatives (13a–g). The precipitates obtained was filtered off, washed with water and recrystallized with ethanol.

(*E*)-***N-[(1,3-diphenyl-1H-pyrazol-5-yl)] methylene)-2-(napthalen-1-yl)-acetohydrazide (13 a)****:* 63%, **mp (℃):** 179-181, **FTIR υmax (cm^{-1}):** 3385 (N–H stretch (hydrazone)), 3004 (C-H str, aromatic), 1673 (C=O str amide), 1537 (C=N str), 1473 (C-C str); 1298 N–N stretch / C–N stretches, 976 (C-H, out of plane bending), 655 (C-H, out of plane bending), **^{1}H NMR:** ($CDCl_3$): *δ 4.06 (s, 2H, -CH2-), 7.33-7.34 (t, 1H, Ar H, J = 7.40 Hz), 7.39-7.43 (m, 4H, aromatic, ring D), 7.46-7.50 (m, 3H, aromatic, ring C), 7.50 (s, 1H, CH-Pyrazole), 7.52-7.54 (d, 1H. ArH, J = 6.85 Hz), 7.64-7.66 (d,1H, ArH, J = 9.25Hz 1.3 Hz), 7.71-7.73 (d, 1H, Naphtyl, J = 8.95 Hz), 7.73-7.74 (d, 2H, naphthyl H) J=7.3 Hz, J = 1.4 Hz), 7.84-7.86 (d, 1H, naphthyl H, J = 7.45 Hz),7.97-7.98(d, 1H, naphthyl H, J = 8.45), 8.06-8.07 (d, 1 H, naphthyl H, J = 7.65 Hz), 7.86 (s, 1H, -CH=N-), 9.41 (s, 1H, NH-).* ***Elemental analyses:*** *Calcd. for $C_{28}H_{22}N_4O$: C, 78.12; H, 5.15; N, 13.01, O, 3.72%.*

(*E*)-***N"-[(3-(4-hydroxyphenyl)-1-phenyl-1H-pyrazol-5-yl)]methylene)-2-(napthalen-1-yl)acetohydrazide (13b)****:* **% Yield:** 63%, **mp (℃):** 220-222, **FTIR υmax (cm^{-1}):** 3375 (N–H stretch (hydrazone)), 3050 (C-H str, aromatic), 1641 (C=O str amide), 1584 (C=N str), 1280 N–N stretch / C–N stretches, 782(C-H, out of plane bending).**^{1}H NMR:** ($CDCl_3$): *δ 3.41 (s, 1H, -OH-), 4.07 ((s, 2H, -CH2-), 6.93-6.95 (d, 2H, Ar (C)), 6.97-6.99 ((d, 2H, Ar (C)), 7.33-7.37 (t, 3H, Ar, (D)), 7.45 (s, 1H, CH-Pyrazole), 7.47-7.49 (d, 2H, Ar (D), J = 10 Hz), 7.52-7.54 (d, 2H, naphthyl H, J = 10 Hz), 7.54 (s, 1H, -CH=N-), 7.61-7.65 (t, 1H, naphthyl H, J = 10 Hz), 7.82-7.86 (t, 1H, naphthyl H), 7.93-7.97 (t, 1H, naphthyl H), 8.07-8.09 (d, 1H, naphthyl H), 8.15-8.17 (d, 1H, naphthyl H), 9.12 (s, 1H, NH-)*

Elemental analyses: *Calcd. for $C_{28}H_{22}N_4O_2$: C, 75.32; H, 4.97; N, 12.55, O, 7.17%.*

(*E*)-***N"-[(3-(4-bromophenyl)-1-phenyl-1H-pyrazol-5-yl)]methylene)-2(napthalen-1-yl)acetohydrazide (13c)****:* **% Yield:** 61%,**mp (℃):** 181-183, **FTIR υmax (cm^{-1}):** 3379 (N–H stretch (hydrazone)), 3185 (C-H str, aromatic), 1654 (C=O str amide), 1550 (C=N str), 1466 (C-C str); 1222 N–N stretch / C–N stretches, 878 (C-H, out of plane bending), 621 (C-H, out of plane bending),**^{1}H NMR:** ($CDCl_3$): *δ 4.13 (s, 2H, -CH2-), 6.93-6.95 (d, 2H, aromatic, ring C), 6.97-6.99 (d, 2H, aromatic, ring C, J = 10 Hz), 7.05-7.08 (d, 2H, aromatic, ring D,), 7.40-7.44 (t, 3H, Ar (ring D)J = 10 Hz), 7.55-7.59 (t, 2H, naphthyl H, J = 10 Hz), 7.57 (s, 1H, -CH=N-), 7.90-7.92 (d, 3H, naphthyl H), 7.97-7.99 (d, 2H, naphthyl H), 9.29 (s, 1H, CH-Pyrazole), 9.92 (s, 1H, NH-)*

Elemental analyses*: Calcd. for $C_{28}H_{21}BrN_4O$: C, 66.02; H, 4.16; Br, 15.69; N, 11, O, 3.14%.*

(*E*)-***N"-[(3-(4-chlorophenyl)-1-phenyl-1H-pyrazol-5-yl)] methylene)-2 (napthalen-1-yl)acetohydrazide (13d)****:* **% Yield:** 60%, **mp (℃):** 175-176, **FTIR υmax (cm^{-1}):** 3261 (N–H stretch (hydrazone)), 3116 (C-H str, aromatic), 1679 (C=O str amide), 1518 (C=N str), 1469 (C-C str); 1345 N–N stretch / C–N stretches, 855 (C-H, out of plane bending), **^{1}H NMR** ($CDCl_3$): *δ 4.13 (s, 2H, -CH2-), 7.37-7.40 (t, 1H, Ar (D), 7.5 Hz), 7.44-7.47 (t, 2H, Ar (D), 7.5 Hz), 7.52 (s, 1H, -CH=N-), 7.55-7.59 (dd, 2H, Ar, (D), , 2H, naphthyl H, J = 10 Hz), 7.80-7.82 (t, 3H, naphthyl), 7.96-7.98 (d, 4H, Ar (C)J = 10 Hz), 8.12-8.14 (d, 1H, naphthyl H, J = 10 Hz), 8.21 (s, 1H,-CH2- pyrazole), 9.00 (s, 1H, NH-),*

ESI-MS: *465 (M+1)*

Elemental analyses: *Calcd. for $C_{28}H_{21}ClN_4O$: C, 72.33; H, 4.55; Cl, 7.63; N, 12.05, O, 3.44%.*

(*E*)-***2-(napthalen-1-yl)-N"-[(3-(4-nitrophenyl)-1-phenyl-1H-pyrazol-5-yl)]methylene)acetohydrazide (13e)***: **% Yield:** 56%, **mp (℃):** 200-204, **FTIR υmax (cm^{-1}):** 3255 (N–H stretch (hydrazone)), 3099 (C-H str, aromatic), 1670 (C=O str amide), 1468 (C-C str); 1291 N–N stretch / C–N stretches, 841 (C-H, out of plane bending), 720 (C-H, out of plane bending), **^{1}H NMR:** ($CDCl_3$): δ *4.05 (s, 2H, -CH2-), 7.49-7.50 (m, 2H, aromatic, ring D), 7.51-7.53 (t, 1H, aromatic, ring D, 5Hz), 7.53-7.54 (m, 2H, aromatic, ring D),7.54 (s, 1H, -CH=N-), 7.78-7.79 (m, 2H, aromatic, ring C),), 7.79-7.80 (m, 2H, aromatic,*

ring C, J = 7.65 Hz), 7.85-7.86 (d, 1H, naphthyl H, J = 7.3 Hz), 7.99-8.00 (d, 1H, naphthyl H, J = 7.65 Hz), 8.15-8.18 (m, 2H, naphthyl H), 8.33-8.35 (dd, 2H, naphthyl H, J = 8 Hz , J =2 Hz), 8.57(s, 1 H, -CH- Pyrazole), 10.8 (s, 1H, NH-)

ESI-MS: 474 (M-1)

Elemental analyses: *Calcd. for $C_{28}H_{21}N_5O_3$: C, 70.73; H, 4.45; N, 14.73, O, 10.09%.*

(*E*)-***N"-[(3-(4-methoxyphenyl)-1-phenyl-1H-pyrazol-5-yl)]methylene)-2-(napthalen-1-yl)acetohydrazide*** **(13f)**: **% Yield:** 53 %, **mp (**℃**):** 182-184, **FTIR** υ_{max} **(**cm^{-1}**):** 3200 (N–H stretch (hydrazone)), 3104 (C-H str, aromatic), 1673 (C=O str amide), 1213 N–N stretch / C–N stretches, 892 (C-H, out of plane bending), 694 (C-H, out of plane bending), **^{1}H NMR:** ($CDCl_3$): *3.81 (s, 3H, -OCH3), 4.06 (s, 2H, -CH2-),6.90-6.92 (d, 1H, aromatic, ring C, J = 8.65 Hz), 6.96-6.97 (d, 1H, aromatic, ring C, J =6.85 Hz), 7.04-7.05 (d, 1H, aromatic, ring C, J = 6.85 Hz), 7.34-7.54 (m, 5H, aromatic, ring D),7.51 (s, 1H, -CH=N-), 7.58-7.60 (d, 1H, naphthyl H , J = 6.75 Hz), 7.67-7.73 (m, 1H, naphthyl H), 7.78-7.79 (t, 1H, naphthyl H), 7.83-7.85-8.00 (t, 1H, naphthyl H), 7.85-7.86 (d, 1H, naphthyl H, J = 8 Hz), 7.99-8.00 (d, 1H, naphthyl H, J = 7.75Hz), 8.19(s, 1 H, -CH- Pyrazole), 10.00 (s,1H, NH)*

ESI-MS: *459 (M-1)*

Elemental analyses*: Calcd. for $C_{29}H_{24}N_4O_2$: C, 75.63; H, 5.25; N, 12.17, O, 6.95%.*

(*E*)-***2-(napthalen-1-yl)-N"-[(1-phenyl-3-p-tolyl-1H-pyrazol-5-yl)]methylene)acetohydrazide (63g)****:* **% Yield:** 65%, **mp (**℃**):** 174-176, **FTIR** υ_{max} **(**cm^{-1}**):** 3284 (N–H stretch (hydrazone)), 3122 (C-H str, aromatic), 1658 (C=O str amide), 1346 N–N stretch / C–N stretches, 901 (C-H, out of plane bending), 624 (C-H, out of plane bending), ***^{1}H NMR: (***$CDCl_3$): *δ 2.51 (s, 3H, -CH3), 4.12 (s, 2H, -CH2-), 7.26-7.28 (d, 2H, aromatic, ring D, J = 10 Hz), 7.33-7.36 (t, 2H, aromatic, ring D, J = 10 Hz), 7.46 (s, 1H, CH- Pyrazole), 7.51-7.57 (q, 4H, Ar ring C, J = 10 Hz), 7.55 (s, 1H, -CH=N-),7.63-7.66 (t, 1H, aromatic ring D, J = 10 Hz), 7.85-7.87 (d, 2H, naphthyl H, J = 10 Hz), 7.94-7.99 (m, 4H, naphthyl H), 9.02 (s, 1H, NH-).*

Elemental analyses: *Calcd. for $C_{29}H_{24}N_4O$: C, 78.36; H, 5.44; N, 12.60, O, 3.60%.*

Antimicrobial evaluation: The antimicrobial activity of all synthesized compounds was evaluated in collaboration with Microcare Laboratory & TRC, an ICMR–NABL–NTEP (formerly RNTCP) approved laboratory, Gujarat, India, using standard microbiological protocols.

Determination of antimicrobial activity by micro-broth dilution method: The antibacterial and antifungal activities of the synthesized compounds were determined by the microbroth dilution method for the estimation of minimum inhibitory concentration (MIC), defined as the lowest concentration of a compound that completely inhibits visible microbial growth. The growth medium was prepared using Mueller–Hinton broth and the test inocula were standardized to approximately 10^8 CFU/mL by turbidity comparison. The turbidity was recorded for each compound in the presence of appropriate controls, including drug control, vehicle control (DMSO), and standard drug control. The microbial strains (MTCC, IMTECH, Chandigarh, India) used for the study are mentioned as *Escherichia coli (*443*), Pseudomonas aeruginosa (*1688*), Staphylococcus aureus (*96*), Streptococcus pyogenes (*442*), Candida albicans (*227*), Aspergillus niger (*282*),* and *Aspergillus clavatus (*1323*).*

Procedure: Stock solutions of test compound (2000 µg/mL) were prepared in DMSO and serially diluted. Primary antimicrobial screening was carried out at the concentrations of 1000, 500, and 250 µg/mL. All test tubes were inoculated and incubated at 37 °C for 18–24 h. The compounds exhibiting inhibitory activity in primary screening were further subjected to secondary screening at 200, 100, 50, 25, 12.5, and 6.25 µg/mL and compared with the control tubes to confirm microbial viability. The lowest concentration that showed complete inhibition of the visible microbial growth is recorded as the MIC.

IC_{50} determination: Linear regression relationship between percentage inhibition and log concentration using the Sakuma method is used to calculate the IC_{50} values and expressed as mean ± standard deviation (SD) of three independent experiments.

In silico **ADMET analysis:** The chemical structures of new hybrids were drawn using ChemDraw and submitted in the online freely available SwissADME https://www.swissadme.ch/ for prediction of pharmacokinetic properties such as lipophilicity, solubility, GI absorption, BBB permeability, and bioavailability, number of hydrogen bond donor (HBD), hydrogen bond acceptor (HBA), rotatable bonds, and TPSA etc. The generated pharmacokinetic data was compiled and analyzed to assess the drug-like behavior of the compounds.

Molecular docking study: Molecular docking was performed to evaluate the binding affinity of the synthesized compounds toward *E. coli* DNA gyrase B (PDB ID: 6F86) using PyRx with AutoDock Vina, and interactions were analyzed using BIOVIA Discovery Studio Visualizer. The protein structure was prepared by removing water molecules, co-crystallized ligands, and heteroatoms, followed by the addition of polar hydrogens and Kollman charges, and saved in PDBQT format. Ligands were drawn in ChemDraw, converted to 3D structures, energy-minimized, and transformed to PDBQT using Open Babel. Docking protocol validation was carried out by re-docking the native ligand into the active site, and an RMSD < 2.0 Å confirmed reliability. The grid box was centered on the active site, and default Vina parameters were applied. For each ligand, the best pose was selected based on the

lowest binding energy. Protein–ligand interactions were analyzed to determine binding modes and key contacts.

CONCLUSIONS: In the present study, a series of new (*E*)-*N*-[(1,3-diphenyl-1*H*-pyrazol-5-yl)methylene]-2-(naphthalen-1-yl)acetohydrazide derivatives were rationally designed, synthesized, and evaluated for their antimicrobial potential. Newly synthesized hybrids exhibited good to moderate antibacterial activity against both Gram-positive and Gram-negative strains. Structure–activity relationships analysis suggested that the nature of substituents on the phenyl ring affects the antibacterial activity among the series. *In silico* studies showed the favorable physicochemical and pharmacokinetic properties of the synthesized hybrids. Further, the results obtained in the molecular docking studies against *E. coli* DNA gyrase B revealed strong binding affinities and stable interactions within the active site, supporting the observed *in vitro* activity.

Conflict of Interest: The authors declare no conflict of interest.

Declaration of funding: No funding was received for this work.

ACKNOWLEDGEMENTS: The authors are thankful to the Department of Pharmaceutical Sciences, Gurugram University for providing necessary facilities to carry out this research work. The authors are also thankful to SAIF, Panjab University, Chandigarh for carrying out the spectral analysis.

REFERENCES

1 Ahmed, S. K.; Hussein, S.; Qurbani, K.; Ibrahim, R. H.; Fareeq, A.; Mahmood, K. A.; Mohamed, M. G. Antimicrobial resistance: Impacts, challenges, and future prospects, *J. Med. Surg. Public Health,* 2024, 2, 100081. https://doi.org/10.1016/j.glmedi.2024.100081

2 Naghavi, M.; Vollset, S. E.; Ikuta, K. S.; Swetschinski, L. R.; Gray, A. P.; Wool, E. E.; Aguilar, G. R.; Mestrovic, T.; Smith, G.; Han, C.; Hsu, R. L. Global burden of bacterial antimicrobial resistance 1990–2021: A systematic analysis with forecasts to 2050, *Lancet*, 2024, 404, 1199-1226. https://doi.org/10.1016/s0140-6736(24)01867-1

3 Salam, M. A.; Al-Amin, M. Y.; Salam, M. T.; Pawar, J. S.; Akhter, N.; Rabaan, A. A.; Alqumber, M. A. Antimicrobial resistance: A growing serious threat for global public health, *Healthcare*, 2023, 11, 1946. https://doi.org/10.3390/healthcare11131946

4 Rusu, A.; Lungu, I. A.; Moldovan, O. L.; Tanase, C.; Hancu, G. Structural characterization of the millennial antibacterial (fluoro)quinolones—Shaping the fifth generation, *Pharmaceutics*, 2021, 13, 1289. https://doi.org/10.3390/pharmaceutics13081289

5 Makar, S.; Saha, T.; Singh, S. K. Naphthalene, a versatile platform in medicinal chemistry: Sky-high perspective, *Eur. J. Med. Chem*., 2019, 161, 252-276. https://doi.org/10.1016/j.ejmech.2018.10.018

6 Alam, M. A. Pyrazole: An emerging privileged scaffold in drug discovery, *Future Med. Chem*., 2023, 15, 2011-2023. https://doi.org/10.4155/fmc-2023-0207

7 Li, G.; Cheng, Y.; Han, C.; Song, C.; Huang, N.; Du, Y. Pyrazole-containing pharmaceuticals: Target, pharmacological activity, and their SAR studies, *RSC Med. Chem*., 2022, 13, 1300-1321. https://doi.org/10.1039/d2md00206j

8 Nehra, B.; Kumar, M.; Chawla, V.; Chawla, P. A. Current progress in synthetic and medicinal chemistry of pyrazole hybrids as potent anticancer agents with SAR studies, *Future J. Pharm. Sci*., 2025, 11, 75. https://doi.org/10.1186/s43094-025-00821-7

9 Boulebd, H.; Zine, Y.; Khodja, I. A.; Mermer, A.; Demir, A.; Debache, A. Synthesis and radical scavenging activity of new phenolic hydrazone/hydrazide derivatives: Experimental and theoretical studies, *J. Mol. Struct*., 2022, 1249, 131546. https://doi.org/10.1016/j.molstruc.2021.131546

10 Kira, M. A.; Abdel-Rahman, M. O.; Gadalla, K. Z. The Vilsmeier-Haack reaction-III cyclization of hydrazones to pyrazoles, *Tetrahedron Lett*., 1969, 10, 109-110. https://doi.org/10.1016/S0040-4039(01)88217-4

11 Attaryan, O. S.; Antanosyan, S. K.; Panosyan, G. A.; Asratyan, G. V.; Matsoyan, S. G. Vilsmeier-Haak formylation of 3,5-dimethylpyrazoles, *Russ. J. Gen. Chem*., 2006, 76, 1817-1819. https://doi.org/10.1134/S1070363206110260

12 Narang, R.; Narasimhan, B.; Sharma, S. (Naphthalen-1-yloxy)-acetic acid benzylidene/(1-phenyl-ethylidene)-hydrazide derivatives: Synthesis, antimicrobial evaluation, and QSAR studies, *Med. Chem. Res*., 2012, 21, 2526-2547. https://doi.org/10.1007/s00044-011-9776-0

13 Molteni, G., Cargnoni, F., Soave, R., & Ponti, A. The (E, Z) Isomerization of C-methoxycarbonyl-N-aryl chlorohydrazones. *Chem.*, 2022, *4*(4), 1624-1653. https://doi.org/10.3390/chemistry4040106

14 Sivaramakarthikeyan, R., Iniyaval, S., Saravanan, V., Lim, W. M., Mai, C. W., & Ramalingan, C. Molecular hybrids integrated with benzimidazole and pyrazole structural motifs: Design, synthesis, biological evaluation, and molecular docking studies. *ACS omega,* 2020, 5(17), 10089-10098. https://doi.org/10.1021/acsomega.0c00630

15 Berwal, P.; Rohilla, S.; Mathur, N.; Rani, K. Synthesis, molecular docking, and biological evaluation of novel indole-triazole conjugates, *Curr. Drug Discov. Technol*., 2024, 21, 115-129. https://doi.org/10.2174/0115701638295739240222074426